Available online at www.sciencedirect.com
SCIENCE DIRECT®
Surface Science 525 (2003) 107–118
SURFACE SCIENCE
www.elsevier.com/locate/susc

Dissociative adsorption of hydrogen on strained Cu surfaces

Sung Sakong, Axel Groß *

Physik Department T30g, Technische Universität München, James-Franck-Straße, 85747 Garching, Germany

Received 7 August 2002; accepted for publication 23 October 2002

Abstract

The adsorption and dissociation of hydrogen on strained clean and oxygen-covered Cu surfaces have been studied by calculations based on density functional theory within the generalized gradient approximation. On all surfaces we find an upshift of the surface d-band center upon lattice expansion. Still there is no general trend in the hydrogen adsorption energies at the high-symmetry sites and the dissociation barrier heights as a function of lattice strain for the low-index Cu surfaces in contrast to the predictions of the d-band model. It turns out that the adsorbate-induced change of the Cu local d-band density of states has to be taken into account in order to rationalize these results. As far as the oxygen-precovered Cu(1 0 0) surface is concerned, the strain-induced change in the hydrogen adsorption energies and dissociation barriers can simply be related to the increased hydrogen–oxygen distance upon lattice expansion.

Keywords: Density functional calculations; Low index single crystal surfaces; Chemisorption; Surface stress; Copper; Hydrogen atom

1. Introduction

An understanding of the microscopic factors determining the reactivity of metal surfaces is of strong current interest since it might lead to the improvement of catalysts in a systematic way [1,2]. In particular, the effect of strain on the surface reactivity has currently been the subject of several studies [3–9]. Substrate strain can strongly modify the surface reactivity, as has recently been shown experimentally [3,4]. By implementing subsurface argon bubbles at a Ru(0 0 0 1) surface, laterally stretched and compressed surface regions have been created. STM images confirmed that oxygen atoms and CO molecules adsorb preferentially in the regions of the expanded lattice [3,4].

These findings have been rationalized [5] within the d-band model [10]. The smaller overlap between the substrate atoms at an expanded transition metal surface reduces the width of the d-band. If the d-band is more than half-filled, charge conservation causes an upshift of the d-band [5,11] which usually leads to a higher reactivity [10]. Industrial heterogeneous catalysts are made of metal nanoparticles supported on metal oxides. The small size of the nanoparticles induces a significant strain on the surfaces compared to low-index single crystal surfaces. Just recently it has been demonstrated that there is a strong correlation between the catalytic activity of binary Cu/ZnO catalysts and the strain of copper in the Cu/ZnO system [7]. Indeed, density functional theory (DFT) calculations of the adsorption and dissociation of O_2 on

* Corresponding author. Tel.: +49-892-891-2355; fax: +49-892-891-4655.
E-mail address: agross@ph.tum.de (A. Groß).

0039-6028/02/$ - see front matter
PII: S0039-6028(02)02550-5

Cu(1 1 1) by Xu and Mavrikakis [6] confirmed that a lattice expansion of the Cu(1 1 1) substrate leads to higher binding energies of atomic and molecular oxygen and to lower O_2 dissociation barriers. Subsequent molecular beam experiments found that uniaxial tensile stress enhances the dissociative adsorption of O_2 on Cu(1 0 0) for initial kinetic energies below 250 meV but suppresses it for higher kinetic energies [9].

On second thoughts, the results of the DFT calculations with respect to the strain effects in the oxygen adsorption energies and barrier heights on Cu(1 1 1) are rather surprising. The d-band of copper is filled which means that a shift of the d-band center upon lattice strain should not be expected. Hence the usual explanation for the higher reactivity of expanded surfaces [5,11] does not seem to be applicable to copper surfaces. In order to investigate the effect of surface strain on the reactivity of copper surfaces in more detail, we have extended the previous study by Xu and Mavrikakis by determining the binding energies and dissociation barriers of hydrogen on clean and oxygen-covered copper surfaces. The hydrogen/copper system has served as a benchmark system for the study of the interaction of molecules with surfaces, both experimentally [12–17] as well as theoretically [18–27], still strain effects in the adsorption have not been studied yet.

Using DFT, we have determined the hydrogen atomic adsorption energies and the dissociation barriers on the low-index Cu(1 1 1), Cu(1 0 0) and Cu(1 1 0) surfaces for three different lateral lattice constants corresponding to a compressed, unstrained and expanded substrate. In order to study the influence of adsorbed oxygen on the interaction of copper with hydrogen, we have performed the corresponding calculations for the O(2 × 2)/Cu(1 0 0) surface.

For all considered surfaces, we find an upshift of the center of the d-band upon lattice expansion. Still there is no general trend in the hydrogen adsorption energies as a function of lattice strain at the high-symmetry sites of the low-index Cu surface in contrast to the predictions of the d-band model [5]. In order to understand the unexpected behavior, the d-band center shift *upon adsorption* has also to be taken into account. Furthermore, the dissociation barriers on Cu(1 1 1) and Cu(1 0 0) also show an opposite behavior as a function of the lattice strain. On the other hand, the change in the hydrogen adsorption energies and dissociation barriers on the oxygen-precovered Cu(1 0 0) surface can be simply related to the increasing hydrogen–oxygen distance upon lattice expansion.

This article is structured as follows. After a brief description of the theoretical methodology used in this work we first discuss the electronic structure of copper surfaces as a function of the lattice strain and describe the predictions of the d-band model. Then the calculated adsorption energies and dissociation barriers will be presented in detail together with a careful analysis of the underlying electronic structure. The paper ends with some concluding remarks.

2. Methods

The DFT calculations have been performed using the Vienna ab initio simulation package (VASP) [28]. The exchange-correlation effects have been described within the generalized gradient approximation (GGA) using the Perdew–Wang (PW-91) functional [29]. The ionic cores are represented by ultrasoft pseudopotentials [30] as constructed by Kresse and Hafner [31]. A cut-off energy of 235 eV has been found to be sufficient for converged results, but results requiring high accuracy have been checked with a 350 eV cut-off. The calculated equilibrium lattice constant, $a_{Cu} = 3.642$ Å, agrees to within 1% with the experimental value of 3.610 Å.

The Cu surfaces are modeled by a slab of four layers for the (1 1 1) surface and five layers for the (1 0 0) and (1 1 0) surfaces. All slabs are separated by 12 Å of vacuum. The energetics of hydrogen adsorption have been determined using (2 × 2) surface unit cells for all considered surface terminations. The two uppermost layers of the slabs have been fully relaxed. Since the Fermi edge lies in a region of a low Cu density of states, it turned out that a relatively fine Monkhorst–Pack **k**-point mesh of 16 × 16 × 1 is necessary to obtain converged energies. In order to determine the strain effects, we have used slabs with lateral lattice

constants of 3.533, 3.642, and 3.715 Å, corresponding to 3% compression, no strain, and 2% expansion, respectively.

The hydrogen adsorption energies are determined via

$$E_{\mathrm{ads}} = E_{\mathrm{slab+H}} - \left(E_{\mathrm{slab}} + \tfrac{1}{2}E_{\mathrm{H_2}}\right), \quad (1)$$

where E_{slab} and $E_{\mathrm{slab+H}}$ are the total energies of the slab without and with the adsorbed hydrogen. For the hydrogen binding energy $E_{\mathrm{H_2}}$ in the gas phase we have taken the calculated GGA value of 4.550 eV. Note that the energy gain upon adsorption corresponds to a negative adsorption energy. In the following, we will denote by atomic binding energy the negative value of the atomic adsorption energy.

In addition, we have determined the barrier for dissociative adsorption E_{b}. From the barrier height E_{b}, the energy barrier for associative desorption along a particular reaction path can be derived via

$$E_{\mathrm{des}} = E_{\mathrm{b}} - (E_{\mathrm{ads}}(\mathrm{H}^{(1)}) + E_{\mathrm{ads}}(\mathrm{H}^{(2)})), \quad (2)$$

where we have taken into account that the desorbing molecules might originate from two inequivalent atomic adsorption sites.

3. Results and discussion

3.1. Electronic structure

In order to analyse and understand the trends in the hydrogen adsorption energies, we have utilized the d-band model as proposed by Hammer and Nørskov [10]. In this model, the interaction between an adsorbate and a transition or noble metal is formally split into a contribution arising from the s and p states of the metal and a second contribution coming from the d-band. The interaction with the sp-bands is assumed to lead to an energy renormalization of the adsorbate energy levels.

In the case of the interaction of hydrogen molecules with metal surfaces, both the renormalized H_2 bonding σ_g and the antibonding σ_u^* states have to be considered. The additional effect of the d-band with respect to the interaction energy is then described by [10]

$$\delta E_{\mathrm{d}}^{\mathrm{H_2}} = -2\frac{V^2}{\varepsilon_{\sigma_u^*} - \varepsilon_{\mathrm{d}}} - 2(1-f)\frac{V^2}{\varepsilon_{\mathrm{d}} - \varepsilon_{\sigma_g}} + \alpha V^2, \quad (3)$$

where f is the d-band filling factor, ε_{d} is the center of the local d-band at the position of the substrate atom, and ε_{σ_g} and $\varepsilon_{\sigma_u^*}$ are the renormalized molecular bonding and antibonding adsorbate resonance, respectively. This means that the whole d-band is assumed to act as a single electronic level located at ε_{d}. The coupling matrix element V depends on the distance between the interacting atoms and usually decreases rapidly with increasing distance. For example, a simple $1/r^3$ dependence has been assumed for the interaction of a hydrogen atom with transition or noble metal atoms [10,11]. If the adsorbate is interacting with nonequivalent substrate atoms, then the right-hand side of Eq. (3) has to be replaced by the corresponding sum over these atoms.

The first term in Eq. (3) describes the energy gain due to the interaction of the H_2 antibonding σ_u^* level with the d-band. This interaction is always attractive since the σ_u^*–d antibonding level whose population would cause a repulsive contribution is too high in energy to become populated. The second term describing the σ_g–d interaction depends on the filling of the d-band. The last term αV^2 reflects the repulsion due to the energetic cost of the orthogonalization.

Since copper has a filled d-band, i.e., the filling factor is $f = 1$, the second term of Eq. (3) vanishes, and the contribution of the d-band to the molecule–surface interaction simplifies to

$$\delta E_{\mathrm{d}}^{\mathrm{H_2/Cu}} = -2\frac{V^2}{\varepsilon_{\sigma_u^*} - \varepsilon_{\mathrm{d}}} + \alpha V^2. \quad (4)$$

In the original presentation of the d-band model [10] a formula equivalent to Eq. (3) was used to estimate the d-band contribution to the atomic adsorption energies which contained the factor $(1-f)$ in the attractive term. However, later it turned out [32,33] that irrespective of the filling factor there is a linear relationship between the d-band center shift and the change in the chemisorption strength of atomic hydrogen on metal surfaces,

$$\delta E_{\mathrm{d}}^{\mathrm{H}} = -\frac{V^2}{|\varepsilon_{\mathrm{d}} - \varepsilon_{\mathrm{H}}|^2}\delta\varepsilon_{\mathrm{d}}. \quad (5)$$

This can be understood in terms of the Newns–Anderson model [32]. The position of the renormalized hydrogen 1s adsorption resonance ε_{H} entering Eq. (5) is a strongly varying function of the distance of the hydrogen atom from the surface according to jellium calculations [34,35]. It drops from 1 eV below the Fermi energy at a distance of 1.2 Å to 6 eV below the Fermi energy at a distance of 0.4 Å. Still, the Newns–Andersen model shows that an upshift of the d-band center causes a stronger bonding of adsorbates with their crucial renormalized adsorption states well below the Fermi level [32], even for a filled d-band.

In Fig. 1, the local d-band density of states of the Cu(1 1 1) surface is plotted. The d-band width decreases for increasing lattice constant, as follows from simple tight-binding considerations due to the reduced overlap. In fact, the d-band center of the uppermost Cu(1 1 1) layer shifts up with increasing lattice constant, in agreement with previous calculations [6]. However, this upshift cannot be explained by the simple argument of charge conservation as in the case of a transition metal with a partially filled d-band. As Fig. 1 indicates, the upper edge of the local Cu d-band at the surface is apparently pinned with respect to the Fermi energy. Because of this pinning the band narrowing causes an upshift of the d-band center.

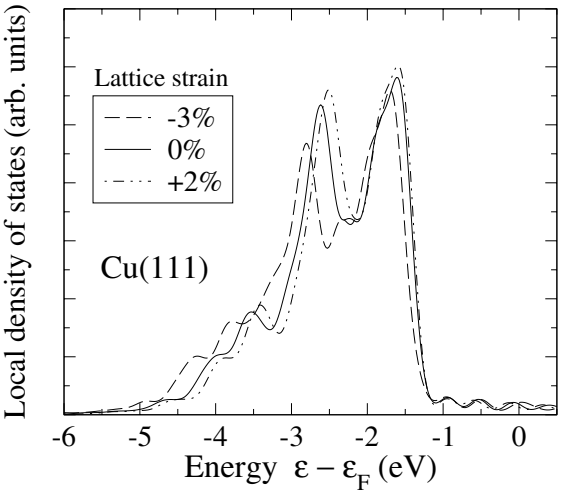

Fig. 1. Local d-band density of states of the Cu(1 1 1) surface as a function of the lattice strain.

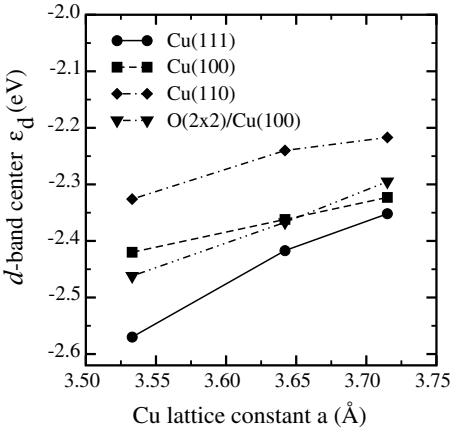

Fig. 2. The d-band center ε_{d} of the surface layer with respect to the Fermi energy as a function of the lattice strain for different copper surface terminations.

The d-band centers ε_{d} as a function of the lattice strain for different Cu surface terminations are plotted in Fig. 2. The first fact that is obvious is that the more open the surface, i.e., the less coordinated the surface atoms, the higher the d-band center. Secondly, the shift of the d-band center is much larger for the Cu(1 1 1) surface than for the Cu(1 0 0) or Cu(1 1 0) surface. The local density of states of the close-packed Cu(1 1 1) surface is much more bulk-like compared to the more open Cu(1 0 0) surface. This demonstrates that the effect of the lattice strain on the electronic structure at an already open, less coordinated surface is less pronounced than for a close-packed surface. The adsorption of oxygen on Cu(1 0 0) also leads to a larger shift of the Cu surface d-band center compared to the pure Cu(1 0 0) surface which can be understood by the fact that the oxygen adsorption increases the effective coordination of the surface copper atoms.

Summarizing the discussion of the electronic structure and reactivity of strained copper surfaces, we would expect that according to the d-band model the atomic hydrogen binding energies on Cu should increase for expanded surfaces while the dissociation barrier should become smaller for

increasing lattice constants which usually leads to a higher reactivity.

3.2. Atomic hydrogen adsorption on Cu

We have determined the atomic hydrogen adsorption energies as a function of the lattice strain at the high-symmetry sites of the Cu(1 1 1), Cu(1 0 0), Cu(1 1 0) and the oxygen-precovered O(2 × 2)/Cu(1 0 0) surfaces. All hydrogen adsorption energies have been obtained for a surface coverage of $\theta_H = 1/4$. For higher hydrogen coverages it turned out that the results were influenced by the mutual repulsive interaction between the hydrogen atoms. For $\theta_H = 1$, we found an increase in the atomic binding energy upon lattice expansion which was simply due to the reduced repulsion between the adsorbates. For the unstrained surfaces, our results compare well with previous calculations in a similar set up within the typical uncertainty of DFT calculations of ±0.1 eV [36,37].

As far as the general site dependence of the hydrogen adsorption energies on the low-index copper surfaces is concerned, we observe that hydrogen prefers to be located at the high-coordination adsorption sites. This is also true for the (1 1 0) Cu surface. Note that the hollow site at the (1 1 0) surface corresponds to adsorption on top of the second layer atom in the trough so that this site is effectively also a low-coordination adsorption site. Now according to the d-band model the interaction between a hydrogen atom and the copper d-band should be repulsive, hence one would not expect that it is energetically favorable to build up many bonds between the hydrogen 1s and the Cu d states. On the other, the delocalized Cu sp states lead to a strong attraction of the hydrogen towards the surface. At the high-coordination sites, the hydrogen atom can minimize its distance to the surface plane while keeping a maximum distance to the nearest Cu atom. This is illustrated in Table 1 where we have listed the height h of the adsorbate position with respect to the uppermost Cu plane and the distances $d_{Cu–H}$ between the hydrogen atom and the nearest Cu atom in addition to the adsorption energies for the Cu(1 1 1) and Cu(1 0 0) surface.

For a quarter monolayer of hydrogen on clean Cu surfaces, there is no clear trend in the atomic adsorption energy as a function of lattice strain, as Fig. 3 demonstrates. On Cu(1 1 1) (Fig. 3a), the adsorption energies at the threefold hollow and the bridge sites are roughly independent of the lattice strain, as expected from the d-band model. At the top site, however, where hydrogen adsorption is

Table 1
Atomic hydrogen adsorption energies E_{ads}, adsorption height h and nearest-neighbor distance $d_{Cu–H}$ between hydrogen and copper on various high-symmetry adsorption sites on Cu(1 1 1) and Cu(1 0 0) as a function of the lattice strain

Lattice constant (Å)	Lattice strain	Cu(1 1 1)										
		fcc hollow			hcp hollow			Bridge			Top	
		E_{ads}	h	$d_{Cu–H}$	E_{ads}	h	$d_{Cu–H}$	E_{ads}	h	$d_{Cu–H}$	E_{ads}	$h = d_{Cu–H}$
3.533	−3%	−0.159	0.976	1.741	−0.152	0.977	1.742	−0.025	1.102	1.666	0.397	1.526
3.642	0%	−0.176	0.919	1.748	−0.165	0.931	1.754	−0.034	1.060	1.668	0.425	1.525
3.715	+2%	−0.166	0.878	1.753	−0.154	0.883	1.751	−0.025	1.032	1.670	0.444	1.527
		Cu(1 0 0)										
		Fourfold hollow			Bridge			Top				
		E_{ads}	h	$d_{Cu–H}$	E_{ads}	h	$d_{Cu–H}$	E_a	$h = d_{Cu–H}$			
3.533	−3%	−0.155	0.638	1.878	−0.061	1.096	1.662	0.339	1.530			
3.642	0%	−0.105	0.544	1.901	−0.025	1.046	1.659	0.420	1.530			
3.715	+2%	−0.079	0.434	1.908	−0.002	1.015	1.660	0.481	1.532			

Energies are given in eV while distances are given in Å.

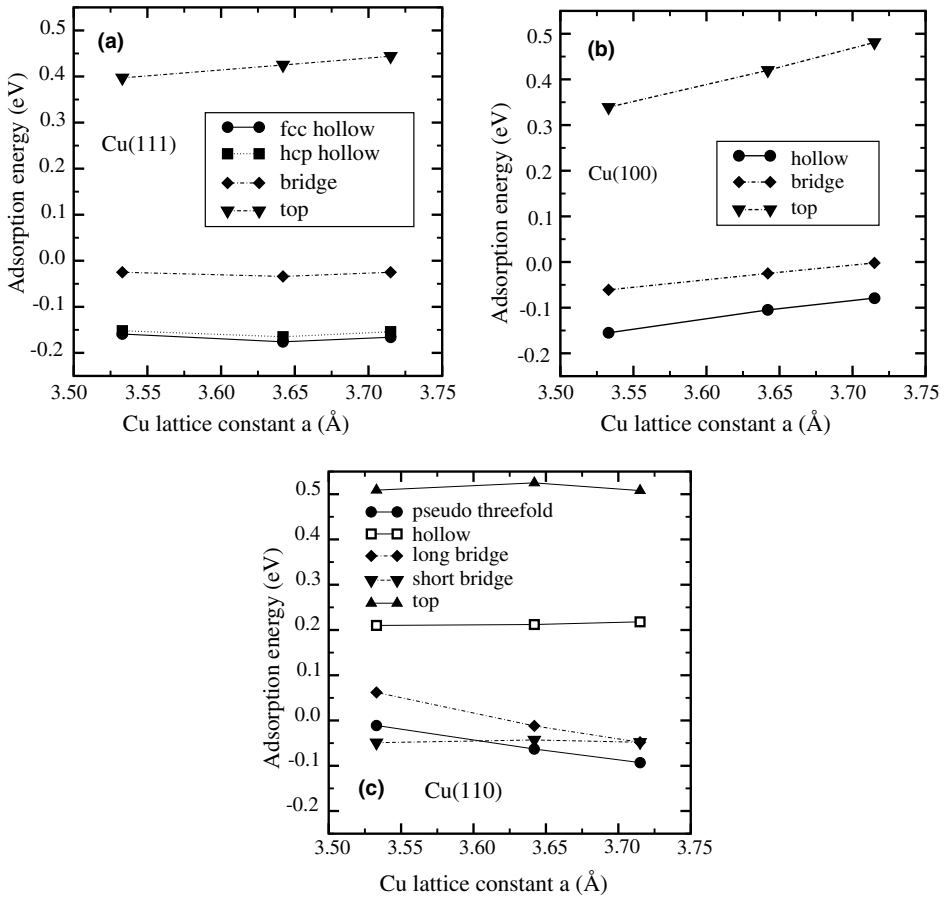

Fig. 3. Atomic hydrogen adsorption energies as a function of the lattice strain at the high-symmetry points of (a) Cu(1 1 1), (b) Cu(1 0 0), (c) Cu(1 1 0).

endothermic with respect to the free hydrogen molecule in the gas phase, we even find a stronger repulsion for the expanded substrate, or in other words, a larger attraction at the compressed surface, in contrast to the trends in adsorption energies as a function of lattice strain usually observed [5,6]. On Cu(1 0 0) (Fig. 3b), this unexpected dependence of the adsorption energies on lattice strain is even obtained at all high-symmetry adsorption sites, whereas on Cu(1 1 0) (Fig. 3c) the binding energies are either constant or increase upon lattice expansion. Apparently, the predictions of the d-band model are only fully confirmed for hydrogen adsorption at the Cu(1 1 0) surface.

In recent molecular beam experiments of the O_2 adsorption on uniaxially stressed Cu(1 0 0) surfaces [9], lattice stress was found to enhance the O_2 adsorption for kinetic energies below 250 meV but to suppress it for energies above 250 meV. Our result that the dependence of the adsorption energies on lattice strain varies between different adsorption sites might provide an explanation for the experiments since at different kinetic energies different regions of the potential energy surface (PES) are probed by the impinging molecules.

The approximate reactivity measure of the d-band model for atomic adsorption Eq. (5) does not only depend on the d-band center but also on the coupling matrix element V which is strongly dependent on the distance between the interacting atoms. We have therefore analysed the change in the adsorbate position as a function of the lattice

strain. As Table 1 demonstrates, at all higher coordinated adsorption sites, the adsorbed hydrogen atom relaxes towards the surface upon lattice expansion. However, this relaxation is done in such a way that the nearest-neighbor hydrogen–copper distance remains basically constant at all considered adsorption site. At the onefold coordinated top site where h and d_{Cu-H} are the same, there is also practically no change in the bond length between hydrogen and copper. Hence we may assume that the coupling matrix elements V also remain basically unchanged upon lattice expansion.

In order to understand the microscopic origin for the unexpected larger H–Cu attraction on the compressed substrate, we have analysed the local density of states upon hydrogen adsorption in more detail. Fig. 4 shows the change of the local density of states of the Cu d-band at the unstrained (1 1 1) surface caused by the hydrogen adsorption on the fcc hollow and the top site, respectively. In addition, the density of states of the hydrogen 1s state is plotted. When the hydrogen atom is adsorbed on the fcc hollow site, the Cu d-band and the H 1s state remain well separated. Furthermore, the Cu d-band is hardly modified by

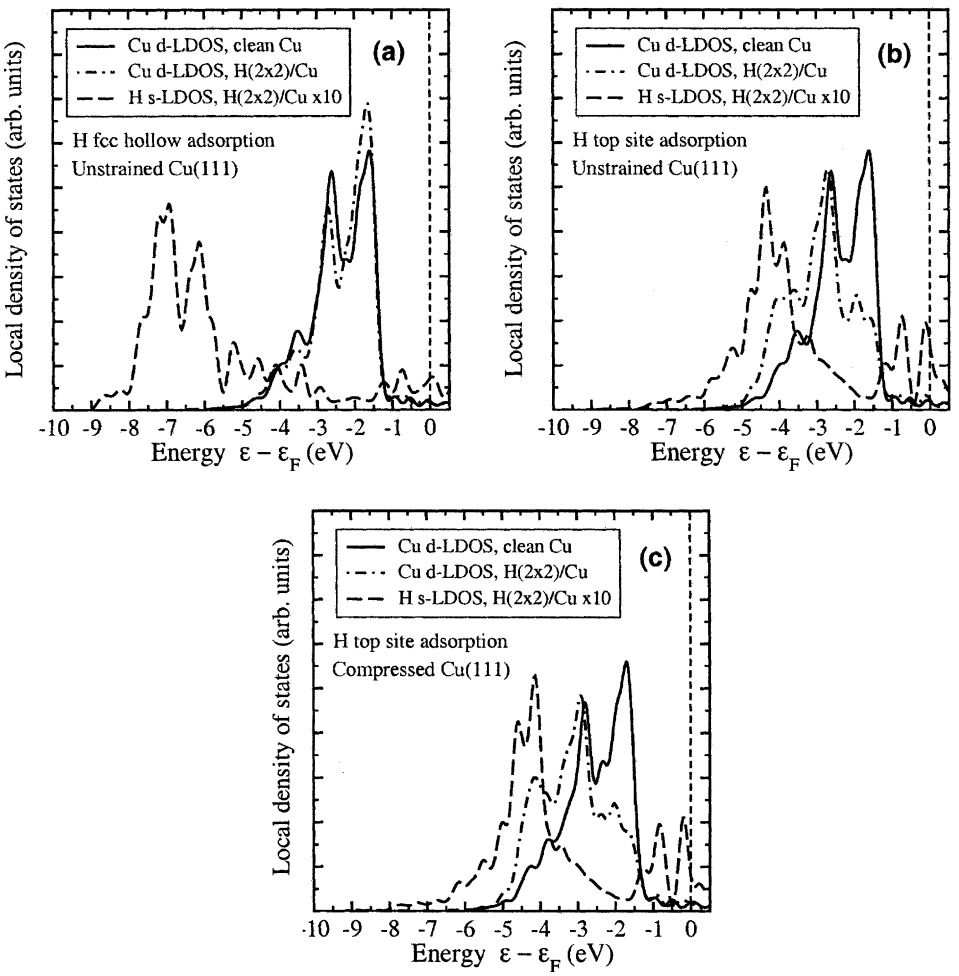

Fig. 4. Local density of states of the hydrogen 1s state and the Cu d-band for atomic hydrogen adsorption on unstrained Cu(1 1 1) at the fcc hollow site (a) and the top site (b) and at the top site for compressed Cu(1 1 1) (c). The hydrogen 1s density of states is multiplied by a factor of 10.

the presence of hydrogen on the surface. Directly above the Cu d-band, the antibonding H 1s–Cu d resonances are visible whose occupation gives rise to the repulsion between the hydrogen atoms and the Cu d bands [38].

For the hydrogen adsorption at the top site, the hydrogen atom is mainly interacting only with one atom directly beneath. In addition, due to symmetry, the hydrogen 1s state only couples to the Cu $d_{3z^2-r^2}$ orbital because all other d orbitals are not rotationally symmetric with respect to the Cu–H bond along the z-axis. Consequently, the H atom at the top site is much more strongly interacting with the single Cu $d_{3z^2-r^2}$ orbital compared to the interaction of the H atom with the Cu d orbitals at the higher coordinated site. This is reflected by the fact that the local d band at the Cu atom beneath the hydrogen atom is strongly modified by the presence of the adsorbate, as Fig. 4 clearly demonstrates, in spite of the fact that only one d orbital is directly involved in the interaction.

Although on the compressed surface the antibonding H 1s–Cu d resonance becomes more occupied leading to an increased repulsion, the adsorbate-induced downshift of the Cu d-band center is larger by 0.15 eV compared to the unstrained surface. This larger downshift overcompensates the increased occupation of the antibonding states thus stabilizing the adsorption at the top site of the compressed Cu(1 1 1) surface.

Consequently, if the hydrogen atom is strongly interacting with a particular copper substrate atom, then apparently the d-band model is no longer fully appropriate. Instead, the response of the local d-band to the presence of the adsorbate has to be taken into account. We find the same phenomenon not only for the onefold coordinated top sites at Cu(1 1 1) and Cu(1 0 0), but also for the twofold coordinated bridge site at the Cu(1 0 0) surface. In fact, for the on-top adsorption of *oxygen* on strained copper surfaces the same unexpected trend as a function of lattice strain is found [6]. An analysis reveals that also for O/Cu(1 1 1) the on-top adsorption leads to a strong perturbation of the electronic structure stabilizing the adsorption on the compressed surface [39].

Surprisingly, the same trend is also observed for the fourfold hollow site at the Cu(1 0 0) surface. However, here the decreasing binding energy upon lattice expansion is caused by another mechanism. For the extended lattice, the hydrogen adsorption position moves closer to the surface plane (see Table 1). This means that the interaction of the hydrogen atom with the second layer copper atom will become stronger. In fact, for an adsorption height of $h = 0$ Å, the distance between the hydrogen atom and the surface copper atom would be the same as the distance to the second layer copper atom leading to an effectively fivefold coordinated adsorption site. The second layer copper atom is already twelvefold coordinated which means that it is rather unreactive. Therefore the reduced distance between the hydrogen atom and the second layer copper atom upon lattice expansion leads to an increased repulsion which is responsible for the lower binding energy [8].

For the (2×2) oxygen-precovered Cu(1 0 0) surface we have also determined the atomic hydrogen adsorption energies as a function of the lattice strain (see Fig. 5). For a quarter monolayer oxygen on Cu(1 0 0) there are two inequivalent fourfold hollow adsorption sites h_1 and h_2. They are indicated in the inset of Fig. 5. As already well-known [23], there is a direct repulsion between oxygen and hydrogen adsorbed on copper surfaces, in other words, oxygen poisons the hydro-

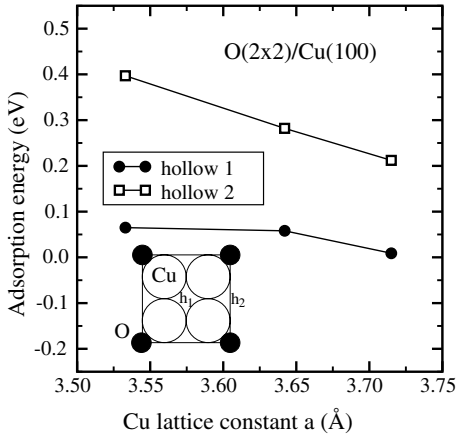

Fig. 5. Atomic hydrogen adsorption energies as a function of the lattice strain at the hollow sites of the $O(2 \times 2)/Cu(1\,0\,0)$ surface. The adsorption sites are indicated by h_1 and h_2 in the inset.

gen adsorption, in particular at site h_2 which is closer to the oxygen atoms than site h_1. Similar results have been found for the hydrogen adsorption on the (2×2) sulfur-precovered Pd(1 0 0) surface [40,41].

In contrast to the clean Cu(1 0 0) surface, we obtain a strong decrease of the adsorption energy upon lattice expansion at the oxygen-covered Cu(1 0 0) surface. As Fig. 2 shows, the d-band center shift is indeed a little bit more pronounced at the oxygen-precovered surface compared to the clean Cu(1 0 0) surface, but not stronger than at the clean Cu(1 1 1) surface. This suggests that it is not the d-band center shift that is responsible for the change in the adsorption energy, but simply the distance between hydrogen and oxygen which increases with the lattice expansion and thus reduces the mutual repulsion. This view is supported by the fact that the change in the adsorption energy is larger at site h_2 that is closer to the oxygen atoms.

3.3. Hydrogen dissociation barriers on copper

In addition to the atomic hydrogen adsorption energies we have also determined the hydrogen dissociation barrier on Cu(1 1 1), Cu(1 0 0) and $O(2 \times 2)$/Cu(1 0 0). At all surfaces, we have kept the center of mass of the hydrogen molecule fixed above the bridge site with the molecular axis parallel to the surface. We have then determined the dissociation path into the adjacent hollow adsorption site by calculating the PES as a function of the H–H interatomic distance d and the center of mass distance from the surface Z in this configuration. Thus the studied dissociation paths correspond to the hollow–bridge–hollow (h–b–h) configuration which is well-known [18,36] to be the most favorable H_2 dissociation path on Cu(1 1 1). At Cu(1 0 0), in fact it has been found that the minimum dissociation barrier can be further reduced by 30 meV by slightly tilting the molecular axis [36]. On $O(2 \times 2)$/Cu(1 0 0), we expect an even stronger energy gain upon tilting from the h_1–b–h_2 configuration because of the inequivalence of the h_1 and the h_2 site.

However, in order to assess the strain effects for similar configurations we did not consider any tilting of the molecular axis in our calculations. The PESs of H_2 dissociation in the h–b–h geometry on unstrained Cu(1 1 1) and Cu(1 0 0) as a function of the H–H distance d and the center of mass distance Z are shown in Fig. 6. It is apparent

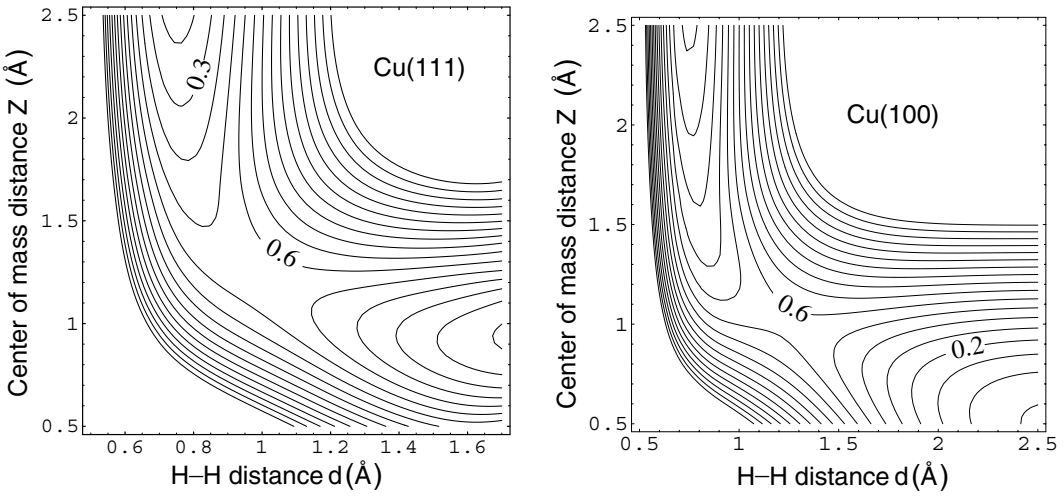

Fig. 6. PES for the hydrogen dissociation on Cu(1 1 1) and Cu(1 0 0) as a function of the H–H interatomic distance d and the center of mass distance from the surface Z. The energy is in eV/molecule, the energy spacing of the contour lines is 0.1 eV. The dissociation path corresponds to the h–b–h geometry, i.e., the center of mass has been kept fixed laterally above the bridge site with the hydrogen atoms dissociating into the neighboring three- or fourfold hollow sites, respectively. Note the different scale of the d axes.

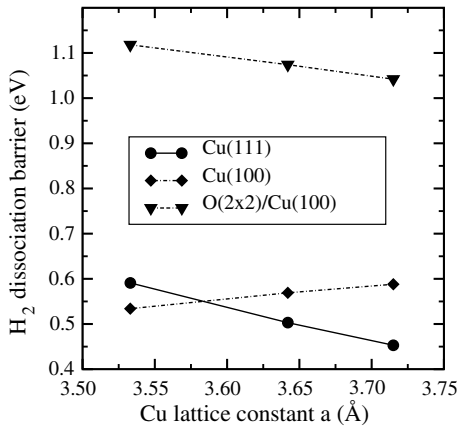

Fig. 7. The H_2 dissociation barrier in the h–b–h geometry (see text) on Cu(1 1 1), Cu(1 0 0) and O(2 × 2)/Cu(1 0 0) as a function of the lattice strain.

that the H_2 dissociation barrier on Cu(1 1 1) is at a larger distance from the surface, but at a closer separation of the two hydrogen atoms, i.e., it corresponds to an *earlier* barrier [21].

The energetic heights of the H_2 dissociation barriers as a function of the lattice strain are plotted in Fig. 7. As far as the unstrained surfaces are concerned, Cu(1 1 1) exhibits the lowest dissociation barrier although the Cu(1 0 0) surface has a higher d-band center than Cu(1 1 1) and should thus be more reactive, i.e., the dissociation barrier should be smaller. This fact has been explained by geometric effects [36]. At Cu(1 0 0), the most favorable atomic adsorption positions, the hollow sites, are farther away from the bridge site than for Cu(1 1 1) so that the transition state to dissociation occurs at a separation of the two hydrogen atoms that is 0.25 Å larger compared to Cu(1 1 1). This is demonstrated in Table 2 where the dissociation and desorption barrier heights E_b and E_{des}, respectively, the H–H distance d and the distance from the surface Z are collected for Cu(1 1 1) and Cu(1 0 0) as a function of lattice strain.

As in the case of the atomic adsorption energies, there is no unique trend of the H_2 dissociation barrier on Cu as a function of lattice strain. For H_2/Cu(1 1 1), the dissociation barrier decreases for increasing lattice constant. This behavior is in accordance with the predictions of the d-band model (Eq. (4)). For Cu(1 0 0), on the other hand, the dissociation barrier increases upon lattice expansion. Thus Cu(1 0 0) shows again a trend that is opposite to the predictions of the d-band model. Indeed we connect this dependence of the dissociation barrier with the trend found for the adsorption energies. Since the dissociation barrier is at a larger separation of the two hydrogen atoms, it is strongly influenced by final states effects, i.e., by the atomic adsorption energies [36]. And since atomic adsorption becomes energetically less favorable at the expanded Cu(1 0 0) surface, the dissociation barrier also increases upon lattice expansion.

Interestingly enough, on Cu(1 0 0) the increase in the dissociation barrier height upon lattice expansion is less pronounced than the increase in the adsorption energies. This can be deduced from the fact that the desorption barrier E_{des} which has been evaluated according to Eq. (2) decreases with increasing lattice constant (see Table 2). On Cu(1 1 1), the desorption barrier also decreases upon lattice expansion but for this surface this mainly stems from the decrease in the dissociation barrier height since the atomic adsorption energies in the Cu(1 1 1) hollow sites are almost independent of small lattice strain (see Fig. 3a).

In a recent DFT study the H_2 dissociation at kink and vacancy defects of Cu surfaces has been

Table 2
Dissociation barrier height E_b, H–H distance d and H_2 distance from the surface Z at the dissociation barrier position and desorption barrier E_{des} on Cu(1 1 1) and Cu(1 0 0) for the hollow–bridge–hollow geometry as a function of lattice strain

Lattice strain	Cu(1 1 1)				Cu(1 0 0)			
	E_b (eV)	d (Å)	Z (Å)	E_{des} (eV)	E_b (eV)	d (Å)	Z (Å)	E_{des} (eV)
−3%	0.581	0.974	1.270	0.892	0.534	1.17	1.080	0.844
0%	0.503	0.971	1.230	0.844	0.569	1.22	1.020	0.779
+2%	0.453	0.987	1.190	0.773	0.588	1.23	0.975	0.746

addressed [27]. Similar to our results, the observed trend in the dissociation barriers did not correlate with the position of the center of the local d-band. An analysis of the electronic structure revealed that in fact changes in the Cu sp states are more important for the modification of the barriers at the defects than changes in the Cu d states. On the basis of our analysis we cannot exclude that there is also an influence of the Cu sp states on the trends found in our study. However, we would expect that any influence of the sp electrons would lead to a unique dependence of adsorption energies and barriers on the substrate strain because of the delocalized nature of the sp electrons. Since we do not find such an unique trend we do not believe that the sp electrons are crucial for an understanding of our results.

As far as the oxygen-covered Cu(1 0 0) surface is concerned, we also find a decrease in the dissociation barrier height with increasing lateral lattice constant, as Fig. 7 shows. However, since this trend is opposite to the one found for the clean Cu(1 0 0) surface, this dependence can again be attributed to the increased distance between hydrogen and oxygen upon lattice expansion which reduces the mutual repulsion.

4. Conclusions

Using DFT, we have studied the dependence of the hydrogen adsorption energies and dissociation barriers on various Cu surfaces as a function of the lattice strain. At all surfaces, the energetic location of the upper edge of the filled copper d-band remains basically fixed when the lateral lattice constant is changed. The band narrowing due to the increase of the lattice constant then causes an upshift of the d-band center. According to the d-band model, this should lead to a stronger atomic binding and to smaller dissociation barriers on the expanded Cu surfaces.

Nevertheless, we find no general trend in the hydrogen/copper interaction energies as a function of lattice strain. Depending on the surface orientation and the adsorption site, hydrogen atomic adsorption energies increase, decrease or remain constant when the lateral lattice constant is varied. In particular at Cu(1 0 0), atomic hydrogen adsorption becomes weaker upon lattice expansion. The smaller atomic binding energies of hydrogen on expanded Cu(1 0 0) also lead to a dissociation barrier that rises with increasing lattice constant. An analysis of the underlying electronic structure reveals that the d-band model is no longer necessarily appropriate when the local density of states at the substrate atoms is strongly perturbed by the presence of the adsorbate which occurs especially at low-coordinated adsorption sites.

On (2×2) oxygen-covered Cu(1 0 0), on the other hand, we find the opposite trend in the hydrogen adsorption energies and dissociation barrier compared to the clean Cu(1 0 0) surface. This is caused by a direct effect, namely the repulsion between hydrogen and oxygen which becomes smaller for a larger separation of the two species.

Finally, in Fig. 8 we compare the change of the hydrogen adsorption energy and dissociation barrier with the oxygen atomic and molecular adsorption energies as well as the transition state (TS) to dissociation on Cu(1 1 1) as a function of the lattice constant. The oxygen data are taken from Ref. [6]. Note that in Ref. [6] a larger lattice strain has been considered.

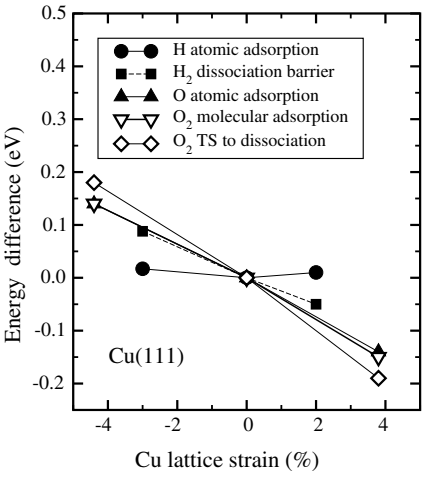

Fig. 8. Change of the hydrogen adsorption energy and dissociation barrier and the oxygen atomic and molecular adsorption energies as well as the transition state (TS) to dissociation on Cu(1 1 1) as a function of the lattice constant. The data for oxygen are taken from Ref. [6].

It is obvious that the atomic hydrogen adsorption energies on Cu(1 1 1) do not follow the trend observed for oxygen on Cu(1 1 1). However, the change of the H_2 dissociation barrier on Cu(1 1 1) caused by substrate strain, although somewhat smaller, is comparable to the change in the oxygen/copper energetics which is in the order of up to 0.2 eV for 5% change in the lattice constant. Thus our calculations confirm that reaction rates on Cu surfaces could be substantially affected by lattice strain.

Acknowledgements

Useful discussions with Bjørk Hammer are gratefully acknowledged. This work has been supported by the German Academic Exchange Service.

References

[1] C. Stampfl, M.V. Ganduglia-Pirovano, K. Reuter, M. Scheffler, Surf. Sci. 500 (2002) 368.
[2] A. Groß, Surf. Sci. 500 (2002) 347.
[3] M. Gsell, P. Jakob, D. Menzel, Science 280 (1998) 717.
[4] P. Jakob, M. Gsell, D. Menzel, J. Chem. Phys. 114 (2001) 10075.
[5] M. Mavrikakis, B. Hammer, J.K. Nørskov, Phys. Rev. Lett. 81 (1998) 2819.
[6] Y. Xu, M. Mavrikakis, Surf. Sci. 494 (2001) 131.
[7] M.M. Günter, T. Ressler, B. Bems, C. Büscher, T. Genger, O. Hinrichsen, M. Muhler, R. Schlögl, Catal. Lett. 71 (2001) 37.
[8] A. Roudgar, A. Groß, Phys. Rev. B 67 (2003), in press.
[9] Y. Uesugi-Saitow, M. Yata, Phys. Rev. Lett. 88 (2002) 256104.
[10] B. Hammer, J.K. Nørskov, Surf. Sci. 343 (1995) 211.
[11] A. Ruban, B. Hammer, P. Stoltze, H.L. Skriver, J.K. Nørskov, J. Mol. Catal. A 115 (1997) 421.
[12] G. Anger, A. Winkler, K.D. Rendulic, Surf. Sci. 220 (1989) 1.
[13] A. Hodgson, J. Moryl, P. Traversaro, H. Zhao, Nature 356 (1992) 501.
[14] M. Gostein, H. Parhiktheh, G.O. Sitz, Phys. Rev. Lett. 75 (1995) 342.
[15] H. Hou, S.J. Gulding, C.T. Rettner, A.M. Wodtke, D.J. Auerbach, Science 277 (1997) 80.
[16] K. Svensson, L. Bengtsson, J. Bellman, M. Hassel, M. Persson, S. Andersson, Phys. Rev. Lett. 83 (1999) 124.
[17] C.T. Rettner, H.A. Michelsen, D.J. Auerbach, J. Chem. Phys. 102 (1995) 4625.
[18] B. Hammer, M. Scheffler, K. Jacobsen, J. Nørskov, Phys. Rev. Lett. 73 (1994) 1400.
[19] A. Groß, B. Hammer, M. Scheffler, W. Brenig, Phys. Rev. Lett. 73 (1994) 3121.
[20] G.R. Darling, S. Holloway, J. Chem. Phys. 101 (1994) 3268.
[21] G.R. Darling, S. Holloway, Rep. Prog. Phys. 58 (1995) 1595.
[22] G.-J. Kroes, E.J. Baerends, R.C. Mowrey, Phys. Rev. Lett. 78 (1997) 3583.
[23] D.M. Bird, Faraday Discuss. 110 (1998) 333.
[24] G.-J. Kroes, Prog. Surf. Sci. 60 (1999) 1.
[25] A. Groß, Surf. Sci. Rep. 32 (1998) 291.
[26] W. Diño, H. Kasai, A. Okiji, Prog. Surf. Sci. 63 (2000) 63.
[27] Ž. Šljivančanin, B. Hammer, Phys. Rev. B 65 (2002) 085414.
[28] G. Kresse, J. Furthmüller, Phys. Rev. B 54 (1996) 11169.
[29] J.P. Perdew, J.A. Chevary, S.H. Vosko, K.A. Jackson, M.R. Pederson, D.J. Singh, C. Fiolhais, Phys. Rev. B 46 (1992) 6671.
[30] D. Vanderbilt, Phys. Rev. B 41 (1990) 7892.
[31] G. Kresse, J. Hafner, J. Phys.: Condens. Matter 6 (1994) 8245.
[32] B. Hammer, O.H. Nielsen, J.K. Nørskov, Catal. Lett. 46 (1997) 31.
[33] V. Pallassana, M. Neurock, L.B. Hansen, B. Hammer, J.K. Nørskov, Phys. Rev. B 60 (1999) 6146.
[34] N.D. Lang, A. Williams, Phys. Rev. B 18 (1978) 616.
[35] H. Hjelmberg, Phys. Scripta 18 (1978) 481.
[36] P. Kratzer, B. Hammer, J.K. Norskøv, Surf. Sci. 359 (1996) 45.
[37] J. Strömquist, L. Bengtsson, M. Persson, B. Hammer, Surf. Sci. 397 (1998) 382.
[38] B. Hammer, J.K. Nørskov, Nature 376 (1995) 238.
[39] Y. Xu, M. Mavrikakis, private communication.
[40] S. Wilke, M. Scheffler, Surf. Sci. 329 (1995) L605.
[41] C.M. Wei, A. Groß, M. Scheffler, Phys. Rev. B 57 (1998) 15572.